Effect of membrane properties on the performance of batch reverse osmosis (RO): The potential to minimize energy consumption

Hosseinipour, E.; Davies, P. A.

DOI:
10.1016/j.desal.2024.117378

Document Version
Publisher's PDF, also known as Version of record

Citation for published version (Harvard):
Hosseinipour, E & Davies, PA 2024, 'Effect of membrane properties on the performance of batch reverse osmosis (RO): The potential to minimize energy consumption', *Desalination*, vol. 577, 117378. https://doi.org/10.1016/j.desal.2024.117378

Desalination 577 (2024) 117378

Contents lists available at ScienceDirect

Desalination

journal homepage: www.elsevier.com/locate/desal

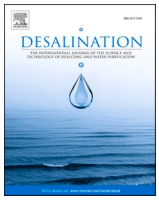

Effect of membrane properties on the performance of batch reverse osmosis (RO): The potential to minimize energy consumption

E. Hosseinipour, P.A. Davies *

School of Engineering, University of Birmingham, Edgbaston, Birmingham, UK

HIGHLIGHTS

- Four 8-in. RO membranes of differing permeabilities tested in free-piston batch RO at recovery of 0.8.
- High-permeability membranes gave 25–29 % lower *SEC* than the low-permeability membrane.
- Predictions indicate up to 30 % *SEC* reduction when permeability further increased from 5 to 20 L/m^2/h/bar.
- Significant differences in osmotic back-flow also observed, from 2.6 to 5.2 L.

GRAPHICAL ABSTRACT

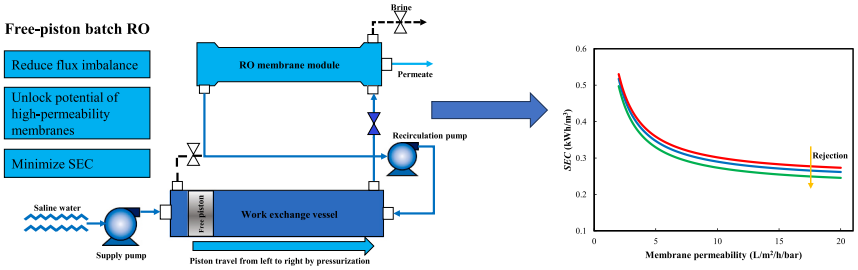

ARTICLE INFO

Keywords:
Batch RO
Membrane permeability
SEC minimization
Salt rejection
Brackish water

ABSTRACT

Efforts to improve the performance of RO desalination include new membranes and new system configurations. Batch RO is an innovative configuration which helps to minimize Specific Energy Consumption (*SEC*) at high recovery. However, there is a lack of experimental studies regarding the performance of different membranes in batch RO. In this study, we tested four 8-in. RO membranes of different permeabilities in a free-piston batch RO system to assess how membrane properties affect performance. Tests were conducted with brackish feed water containing 1000–5000 mg/L of NaCl, at recovery of 0.8. Performance in terms of *SEC*, permeate quality and salt rejection was quantified. *SEC* and salt rejection varied considerably from low-permeability to high-permeability membranes. For the lowest permeability membrane rejection was >95 %, whereas for the higher permeability membranes it was only 82–96 %. *SEC* with high-permeability membranes was approximately 25–29 % lower than with the lowest permeability membrane. Using a verified model, we predict that on increasing the permeability from 5 to 20 L/m^2/h/bar, hydraulic *SEC* would go down further by 17–28 % using ultra high-permeability membranes. Though this study shows the potential for *SEC* reduction, it also underlines the limitations of current commercial membranes and therefore the need for membranes with even higher permeability.

1. Introduction

Membrane reverse osmosis (RO) dominates the desalination industry

Abbreviations: Aq-U, Aquaporin-ultra membrane; BWRO, Brackish water reverse osmosis; CF, Concentration factor; D-HR, Dupont-BW30HR membrane; D-XLE, Dupont-XLE membrane; ICP, Internal concentration polarization; RO, Reverse osmosis; *SEC*, Specific energy consumption; SI, Supporting information; TDS, Total dissolved solids; TFC, Thin film composite; T-TMHA, Toray-TMH20A membrane.

* Corresponding author.
E-mail address: p.a.davies@bham.ac.uk (P.A. Davies).

https://doi.org/10.1016/j.desal.2024.117378
Received 18 November 2023; Received in revised form 22 January 2024; Accepted 22 January 2024
Available online 26 January 2024

Nomenclature

Symbols

c_{feed}	mg/L, feed concentration to the batch RO system
c_{perm}	mg/L, permeate concentration
r	-, recovery
J_w	L/m^2/h, water flux
R_s	-, salt rejection
η	-, second law efficiency
π_{feed}	bar, feed osmotic pressure

today, providing nearly 100 million m^3 of clean water per day globally [1]. Since its introduction in the 1950s, RO desalination has undergone substantial advances in materials science, process refinement, system optimization, techniques for membrane synthesis, and membrane surface modifications [2]. Over the last 3 decades, the specific energy consumption (*SEC*) of RO has almost halved [3]. Driven by the large uptake of RO desalination, research efforts to achieve further advances are on-going.

1.1. Membrane materials and structures

One important research area aims to develop new membrane materials and structures with improved properties such as water permeability and salt selectivity. The polyamide thin-film composite (TFC) is the most common type of membrane, thanks to its high permeability, high salt rejection, stability and low cost [4]. Typically, permeability of current TFC membranes ranges from 1 to 2 L/m^2/h/bar for seawater membranes and 2–8 L/m^2/h/bar for brackish water RO (BWRO) membranes [5]. Conversely, salt rejection is about 99 % for seawater [2,6] and 95–99 % for brackish water [7].

Though the structure of TFC membranes can be modified to enable faster water permeation, such modification also tends to increase the ease of salt passage [8]. This trade-off between permeability and salt rejection, along with the issue of membrane fouling, has posed challenges to the efficient use of RO technology – thus prompting research into alternative membranes. Examples include inorganic membranes consisting of ceramics or 2D-carbon-based materials such as carbon nanotubes and graphene oxides [9]. Inorganic membranes offer advantages including improved chemical and physical stability, as well as high tunability and reusability compared to polymeric membranes. However, their commercialization has been hindered by challenges in preparation, high manufacturing costs, and their thickness and bulkiness [4]. Combining the advantages of both polymeric and ceramic membranes, mixed matrix membranes are another option [10]. In this hybrid organic–inorganic approach, the properties of a polymeric matrix are enhanced by the addition of inorganic fillers. The fillers can be a porous and/or nonporous material such as zeolite, activated carbon, carbon nanotubes, silica, alumina, silver, and/or titanium oxide nanoparticles. However, the application of mixed-matrix membranes is restricted by factors like identification of filler material for synthesis, complex fabrication process, high cost, agglomeration, and phase separation [11].

A further alternative is biomimetic membranes. Biological water channels based on aquaporin proteins promise to enable membranes with exceptional permeability and salt rejection capabilities [12,13]. For instance, Sharma et al. [14] reported membrane permeability in the range of 3–10 L/m^2/h/bar and salt rejection ranging from 90 to 95 % for aquaporin-based membranes fabricated using *E. coli* aquaporin Z proteoliposomes immobilized in a polyamide layer formed by interfacial polymerization. However, current research has yet to provide performance data surpassing that of conventional state-of the-art TFC desalination membranes [15].

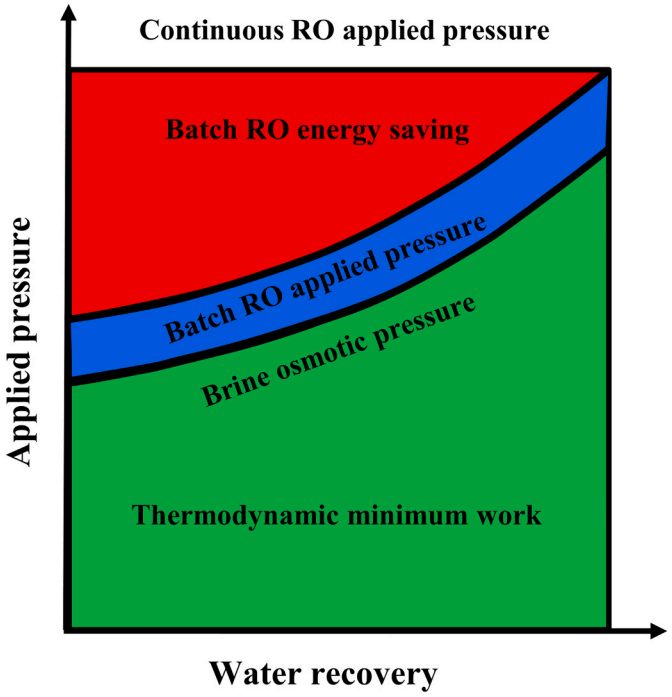

Fig. 1. Comparison of applied pressure vs. water recovery ratio between batch RO and single-stage continuous RO (adapted from [33]). The areas beneath the green, blue, and red curves represent energy.

The extent to which membrane properties influence system performance varies among studies. For example, in a theoretical study, Cohen-Tanugi et al. [16] found that increasing permeability from 1.5 to 4.5 L/m^2/h/bar resulted in a large decrease (46 %) in the feed pump pressure and *SEC* in conventional single-stage BWRO at recovery of 0.65. However, beyond this point, further increases in permeability yielded diminishing returns, with 5 L/m^2/h/bar being considered as the upper limit for meaningful reduction in *SEC* for BWRO.

In another theoretical study, Werber et al. [17] assessed the effect of increasing permeability on energy efficiency in BWRO (at feed concentration of 5844 mg/L NaCl and recovery of 0.75). In a single-stage continuous RO process, a permeability increase from 4 to 10 L/m^2/h/bar yielded a marginal 2.2 % decrease in *SEC*. In contrast, in a two-stage RO configuration (where the energy requirement at 4 L/m^2/h/bar was already 22 % lower than in single-stage RO) an increase in permeability from 4 to 10 L/m^2/h/bar led to a more significant 12 % reduction in *SEC*.

1.2. Configurations for minimal SEC

Traditionally, a single-stage configuration was the norm for RO. However, in the past twenty years, there has been a shift towards multi-stage RO to minimize *SEC* [18]. Wei et al. [19], theoretically assessed the potential energy savings in a two-stage BWRO system using high-permeability membranes (3 and 10 L/m^2/h/bar) at a feed concentration of 3000 mg/L NaCl and recovery rate ranging from 0.60 to 0.98. They found that at lower recoveries, the *SEC* reduction achieved by employing a 10 L/m^2/h/bar membrane is limited (0.02 kWh/m^3 at recovery of 0.6). At very high recoveries (>0.98), *SEC* became almost insensitive to permeability. The highest *SEC* savings due to increased permeability were predicted at recovery of 0.91. They explained that raising the membrane water permeability from 3 to 10 L/m^2/h/bar does not notably enhance energy efficiency, because of growing concentration polarization. They also concluded that the energy savings derived from increased membrane water permeability decline as feed concentration rises.

Although *SEC* tends to bottom out at high permeability, this

tendency varies with process factors like feed concentration, recovery, pump efficiency, and system configuration. Nevertheless, according to Okamoto and Lienhard [3], across all scenarios, any further reduction in energy becomes marginal once the water permeability surpasses approximately 3 and 8 L/m^2/h/bar in seawater and brackish water RO, respectively. This is almost the upper value for the BWRO membranes in the market today, suggesting that improvement in this area is unnecessary for conventional continuous RO.

In contrast to continuous RO, batch RO is an innovative configuration developed to achieve high recovery with reduced energy consumption [20–23]. In a batch RO system, concentration at the membrane varies over time. Meanwhile, applied pressure follows the osmotic pressure helping to minimize *SEC* [24–27]. This contrasts with continuous RO where the constant applied pressure must be maintained at a maximum value as needed to at least overcome the osmotic pressure of the brine corresponding to the recovery of the system (see Fig. 1) [28]. Not only does this excess pressure correspond to wasted energy, but it also results in loss of membrane permeability since several studies have shown decrease of permeability with pressure [29–32].

Understanding factors, such as membrane permeability, that affect *SEC* in batch RO systems is vital for optimizing system performance and energy efficiency. Further research and investigation in this area will contribute to the development of better membrane materials and improved operational strategies for batch RO system designs. To date only a few studies have addressed these issues.

For example, Warsinger et al. [34] theoretically evaluated the impact of permeability on *SEC* in batch RO for seawater (recovery of 0.5 and concentration of 35,000 mg/L) and brackish water (concentration of 5000 mg/L and recovery of 0.66). They assumed an 80 % pump efficiency, and an average membrane flux of 14.5 L/m^2/h. For seawater, most energy savings (~13 %) resulting from more permeable membranes were predicted to occur up to a permeability of 4 L/m^2/h/bar. In the case of brackish water, energy savings (37 %) remained significant up to about 7 L/m^2/h/bar. Beyond these permeability values, a 10 % increase in membrane water permeability yielded <2 % energy saving.

Swaminathan et al. [35] similarly studied the impact of increased permeability on *SEC* in seawater batch RO as compared to traditional continuous seawater RO. They predicted a drop in *SEC* of approximately 10 % (0.2 kWh/m^3) when permeability increases from 2 to 10 L/m^2/h/bar. In continuous RO, the decrease in *SEC* was a more modest 5 % (0.11 kWh/m^3). The study anticipated that batch RO systems may benefit more than continuous RO from the use of ultra-permeable membranes such as those based on graphene or aquaporins.

Hosseinipour et al. [27] tested a batch RO system using an Eco Pro-440 membrane with brackish water at recovery of 0.8 and used the results to calibrate a model. By increasing the permeability from the experimental baseline of 4.4 L/m^2/h/bar up to 10 L/m^2/h/bar, they predicted a *SEC* reduction of 17 % (0.352 down from 0.423 kWh/m^3). These predictions assumed a feed concentration of 4000 mg/L and flux of 17.3 L/m^2/h.

In summary, there have been promising predictions concerning the use of high-permeability membranes to improve performance in batch RO. Compared to continuous RO, high permeability membranes are expected to have a more significant impact on *SEC* in batch RO, and the relative impact is expected to be even larger at lower feed salinities. However, still there is a lack of experimental research in this area. This study sets out to address this gap by testing a batch RO system with a series of state-of-the-art RO membranes, including a recently introduced membrane using biomimetic aquaporin technology. Four 8-in. RO modules with varying permeability were assessed in a single-acting free-piston batch RO pilot. Salt rejection and *SEC* were measured to analyse the trade-off between permeability and selectivity. The validated model was then employed to assess potential *SEC* improvements by enhancing membrane permeability, considering salt rejection within the range of 87–97 %.

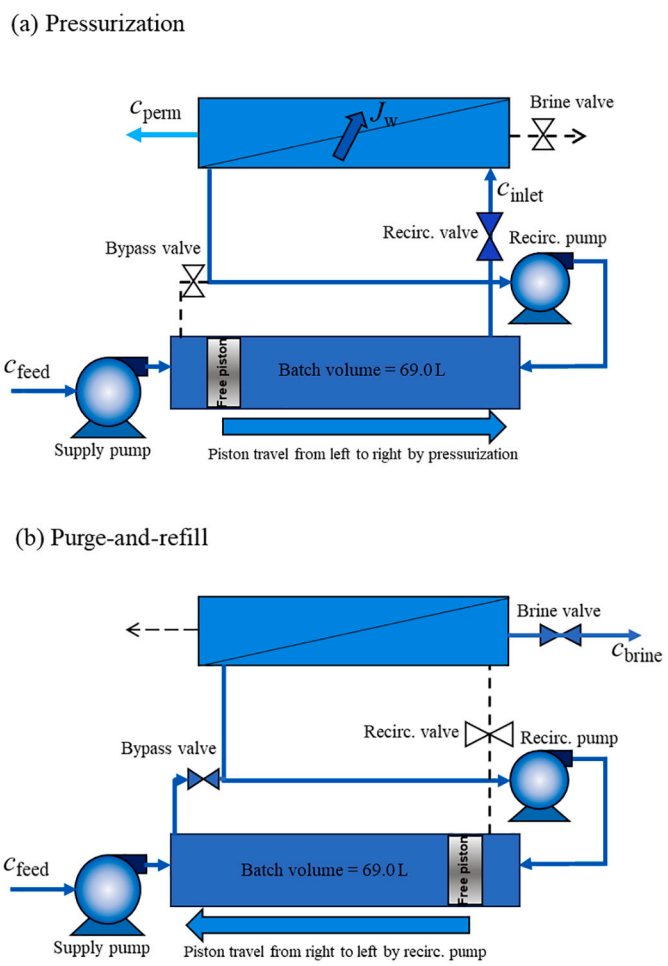

Fig. 2. Schematic of the free-piston batch RO, a) pressurization, and b) purge-and-refill phase. The phases involve switching three on-off valves. In the pressurization phase, the bypass and brine valves are closed while the recirculation valve remains open. Conversely, in the purge-and-refill phase, the bypass and brine valves are open, and the recirculation valve is closed. For more details refer to [27]. Solid and dashed lines represent flow and no flow respectively.

2. Experimental equipment and procedure

This study used a free-piston batch RO system housing a single 8-in. spiral wound membrane (Fig. 2). The system has a maximum rated pressure of 25 bar. Detailed information about the equipment and experimental procedure has been documented in an earlier study [27] and is not repeated here. The earlier study established that, for feed concentrations ≤5000 mg/L, the optimal ratio of recirculation to feed flow is approximately 2 to minimize the *SEC*. To avoid repetition, we used the same ratio here and did not re-evaluate the effect of varying it. This helped to rationalize the number of experiments and provide comparable results.

Four different 8-in spiral-wound RO membranes were tested. Henceforth, these membranes are referred according to the abbreviations in Table 1, which also shows important manufacturers' data. All four membranes are intended for brackish water treatment with maximum pressure of 41 bar (except the T-TMHA membrane which is rated at only 25 bar). Three of these membranes are regarded as high-permeability membranes (Aq-U, D-XLE and T-TMHA) and one as low-permeability and high-rejection (D-HR).

Feed solutions were prepared by dissolving approximately 1.5 to 7.5 kg of reagent grade NaCl (Fisher Scientific, ACS grade, 99.5 % purity) in tap water with total dissolved solids (TDS) < 100 mg/L in a 1500 L

Table 1
Specifications of the 8-in. spiral wound membranes used in this study according to the manufacturers' datasheets. All membranes had area of 41 m^2 and feed spacer thickness of 0.71 mm (0.028 in.). All reported test conditions were at 25 °C, pH = 7–8 and water recovery of 0.15.

Membrane manufacturer and type	Abbreviation	Salt rejection %	Product flow rate (m^3/day)	Maximum operating pressure (bar)	Membrane test conditions		
					Feed concentration, c_{feeed} (mg/L)	Pressure, P_f (bar)	Flux, J_w (L/m^2/h)
Aquaporin-Ultra	Aq-U	99.0	51	41.4	500	6.9	52.1
Dupont-XLE	D-XLE	99.0	53	41.4	2000	8.6	53.9
Dupont-BW30HR	D-HR	99.7	48	41.4	2000	15.5	48.8
Toray-TMH20A	T-TMHA	99.3	45.7	25.1	500	6.9	46.4

Table 2
Membrane water permeabilities measured experimentally and calculated using manufacturers' datasheets. The permeability was calculated using $A = \frac{J_w}{P_f - \pi_f}$ (where P_f and J_w are taken from Table 1 and π_f is calculated using the van 't Hoff expression).

Membrane	Permeability, A (L/m^2/h/bar)	
	Experimental	Calculated
T-TMHA	5.7	7.1
Aq-U	5.4	8.0
D-XLE	4.6	7.7
D-HR	2.7	3.5

polyethylene feed tank, representing brackish water with TDS ranging from 1000 to 5000 mg/L. To remove free chlorine, 4.5 mg of sodium metabisulfite was added to the feed tank. The feed water temperature was kept constant at 25 ± 0.5 °C throughout. A 5-μm 10-in cartridge pre-filter was used to remove small particles and protect the RO membrane.

The system was operated at the design recovery of 0.80 ± 0.01. Experiments were conducted at fluxes ranging from approximately 11–23 L/m^2/h, resulting in an output of 10–17 m^3/day. This translated to a complete cycle duration ranging from 330 to 580 s (including a 75-s purge-and-refill phase), with shorter durations correlating with higher water fluxes. Hence, the overall duration for each run (four cycles) varied from 22 to 44 min. During the experiments, all relevant parameters (shown in Table S1) including conductivities, pressure, flow rates, power consumption of the pumps, and weights of the tanks were monitored and recorded using a data logger and LabVIEW® software. These data were used to calculate results, including *SEC*, salt rejection, and permeate quality – following the calculation methods described previously [27].

The main measurement equipment used in this study (shown in Fig. S8), including pressure sensors, conductivity sensors, power supply, and scales, have errors of <1 % of their respective ranges (0.25 %, 1.0 %, 0.1 %, and 0.3 %, respectively). When considering the cumulative errors, the calculation error for parameters such as salt rejection, hydraulic and electrical *SEC*, and flux falls within the range of 1–3 % in all cases.

3. Result and discussions

3.1. Membrane water permeability

We measured the permeability for each membrane under similar conditions. To eliminate osmotic pressure, RO permeate with a conductivity of approximately 0.1 mS/cm was collected and then used as feed. The pressure and flow rate during the tests were stable, with minimal fluctuations of no more than ±0.1 bar or ± 0.1 L/min respectively. These tests were done in the continuous RO mode operation with the brine valve fully closed (i.e., as a dead-end flow system).

To determine flux, we measured the mass of the produced permeate over a period of 600 s, using a precision scale with an accuracy of ±0.1 kg. The test was repeated over a range of flow and pressure, and the permeability was determined from the slope of the straight-line fit of flux vs. pressure (see SI section 2 for detailed results). For the high-permeability membranes, measured permeability ranged from 4.6 to 5.7 L/m^2/h/bar, while the high-rejection membrane (D-HR) exhibited a permeability of only 2.7 L/m^2/h/bar (Table 2).

Table 2 shows that the experimental values for permeability are lower than those inferred from the manufacturers' datasheets. Nonetheless, such differences are also reported elsewhere in the literature. For example, Khunnonkwao et al. [36] mentioned permeability of about 5 L/m^2/h/bar for the D-XLE membrane, while another study reported

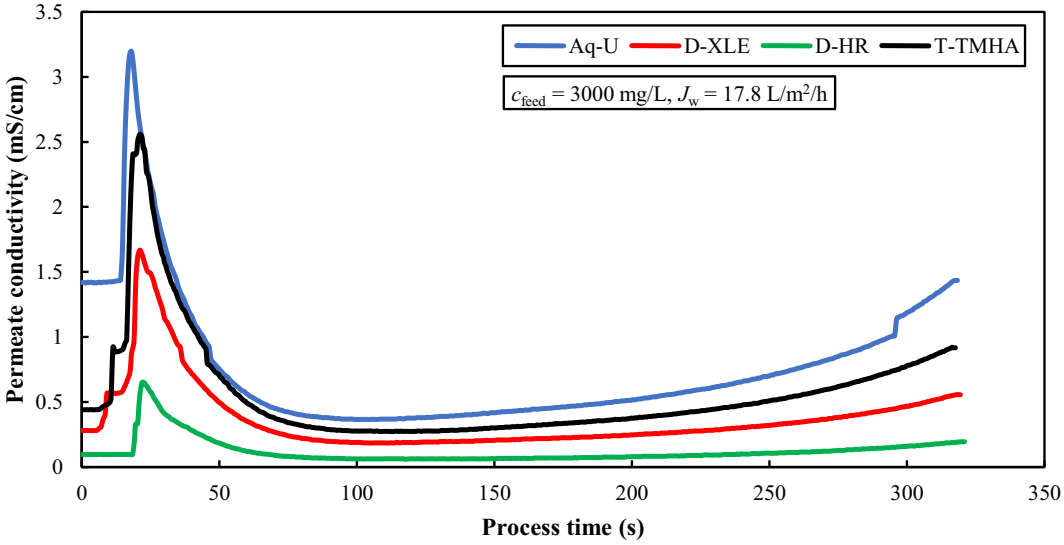

Fig. 3. Permeate conductivity vs. time over the pressurization phase in batch RO at c_{feed} = 3000 mg/L and J_w = 17.8 L/m^2/h for different RO membranes.

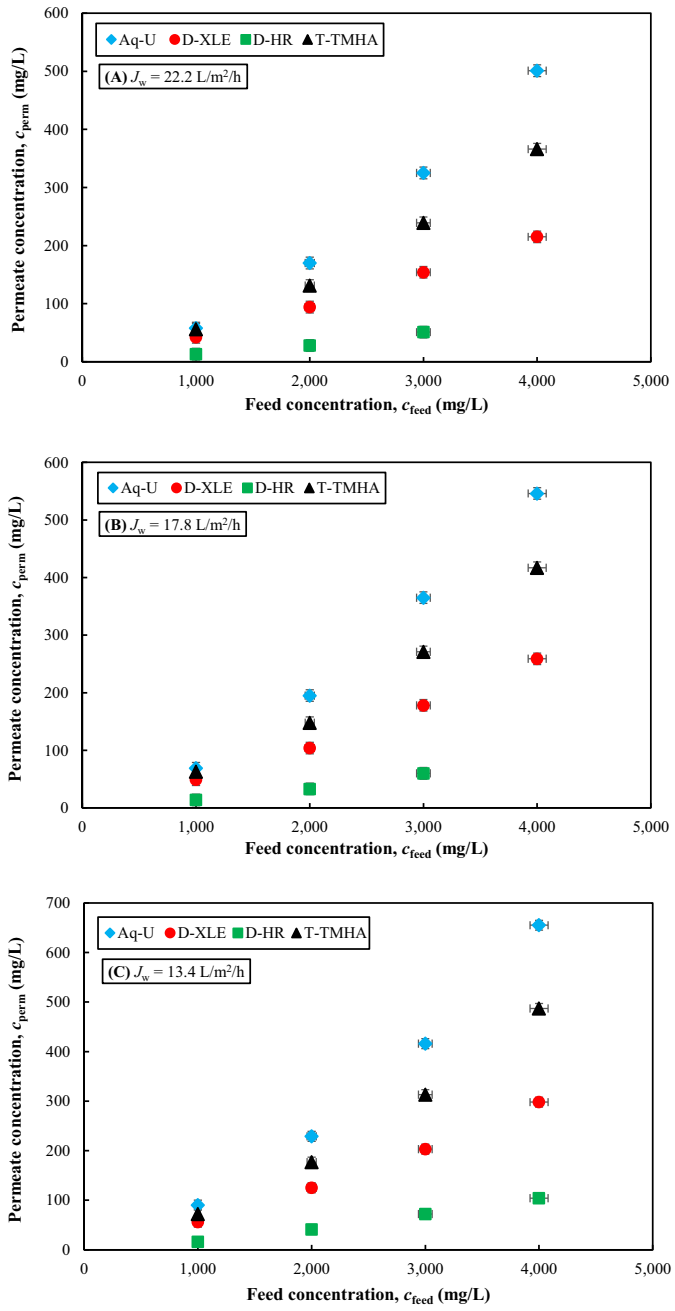

Fig. 4. Average permeate concentration over a cycle in batch RO vs. feed concentration for different RO membranes at A) J_w = 22.2 L/m^2/h, B) J_w = 17.8 L/m^2/h, and C) J_w = 13.4 L/m^2/h.

permeability for this membrane of 3.6 to 6.8 L/m^2/h/bar, depending on the experimental conditions such as pressure [37]. These differences could be due to quality variations in membranes and variations in operating conditions and testing arrangement. In the case of the Aq-U membrane, we note that this is a newly available membrane so its specifications may not yet have been firmly established.

3.2. Permeate conductivity variation over the pressurization phase

Fig. 3 compares permeate conductivity over a pressurization phase. There is an initial delay of about 10–20 s before permeate production commences. During this period, the applied pressure rapidly increases to reach the feed solution's osmotic pressure, before driving water through the membrane. Simultaneously, the permeate spacer and permeate tube, which were previously emptied during the purge phase due to osmotic backflow, are re-filled with water. Next there is a sharp peak in permeate conductivity, like that reported in previous studies [24–27]. This peak indicates that the stagnant salt (that had been drawn into the membrane support layer during the purge phase) is now leaving the system, causing a temporary increase in permeate conductivity. After the peak, the permeate conductivity drops to a minimum, and then it starts to increase steadily as the process continues. This second rise is attributed to the increasing concentration of salt in the recirculation loop of the batch RO system, some of which diffuses across the membrane.

The Aq-U membrane showed the largest initial peak whereas the D-HR showed the smallest. Following the initial peak, the permeate conductivity with the D-HR increased from 0.07 to 0.19 mS/cm during a test at c_{feed} = 3000 mg/L and J_w = 17.8 L/m^2/h. In contrast, D-XLE, T-TMHA, and Aq-U gave greater increases in permeate conductivity from 0.22 to 0.56, 0.32 to 0.91, and 0.4 to 1.43 mS/cm respectively.

The World Health Organization (WHO) generally considers water with a TDS level of less than approximately 600 mg/L to have good palatability [38]. Thus, we compared against this limit. Fig. 4 shows the average permeate concentration over a cycle at different feed concentrations ranging from 1000 to 4000 mg/L, at three different fluxes. The permeate water produced by all membranes at feed concentrations up to c_{feed} = 4000 mg/L met acceptable water quality standards for drinking applications.

Permeate TDS increased with both flux and feed concentration (see Fig. 4). The high-rejection D-HR membrane stood out by consistently producing water with TDS levels below 100 mg/L. This suggests that this membrane offers significant flexibility, allowing for operation at higher feed concentrations and lower fluxes without having to worry about exceeding the TDS limit for drinking applications. Additionally, the D-XLE produced permeate with TDS < 300 mg/L under the same conditions. Both the T-TMHA and Aq-U membranes demonstrated good performance at low feed concentrations ($c_{feed} \leq$ 2000 mg/L). Nonetheless, as the feed concentration increased, the difference in permeate TDS between these two membranes and the D-HR and D-XLE membranes became more noticeable, increasing the risk of failing to meet drinking quality standards. This suggests that the selection of the right membrane should be based on the feed concentration and the final permeate quality required in each application.

The best permeate quality was observed at the highest flux and the lowest feed concentration (J_w = 22.2 L/m^2/h and c_{feed} = 1000 mg/L), resulting in TDS < 60 mg/L for all membranes. The worst permeate quality was seen at the highest feed concentration and the lowest flux. Flux had a big effect on the permeate quality; for example, at c_{feed} = 4000 mg/L and J_w = 13.4 L/m^2/h the average permeate TDS levels were 104, 298, 487, and 655 mg/L for D-HR, D-XLE, T-TMHA, and Aq-U respectively. On increasing flux to J_w = 22.2 L/m^2/h these values reduced by approximately 25 %.

Moreover, the initial conductivity peak (as shown in Fig. 3) has a negative impact on the permeate quality. This peak tends to become more prominent at higher fluxes and feed concentrations. If it did not occur, the permeate TDS levels for the D-XLE, T-TMHA, and Aq-U membranes would have been lower. For instance, at c_{feed} = 4000 mg/L and J_w = 22.2 L/m^2/h, the permeate TDS would have decreased from 215, 366, and 500 mg/L to about 173, 297, and 437 mg/L, respectively. These estimated decreases are based on comparing against a hypothetical situation where the initial permeate concentration is assumed to be at the minimum concentration observed, which is a plausible assumption in the absence of osmotic backflow.

Considering the trade-off between permeate quality and energy efficiency when varying the flux, for the high-permeability membranes, it is recommended to operate the system at higher fluxes whenever possible, even though it may lead to higher energy consumption. By doing so, the improved water quality and permeate output achieved at higher fluxes justifies the increase in energy usage and offers a practical approach to obtain desirable permeate quality for drinking water

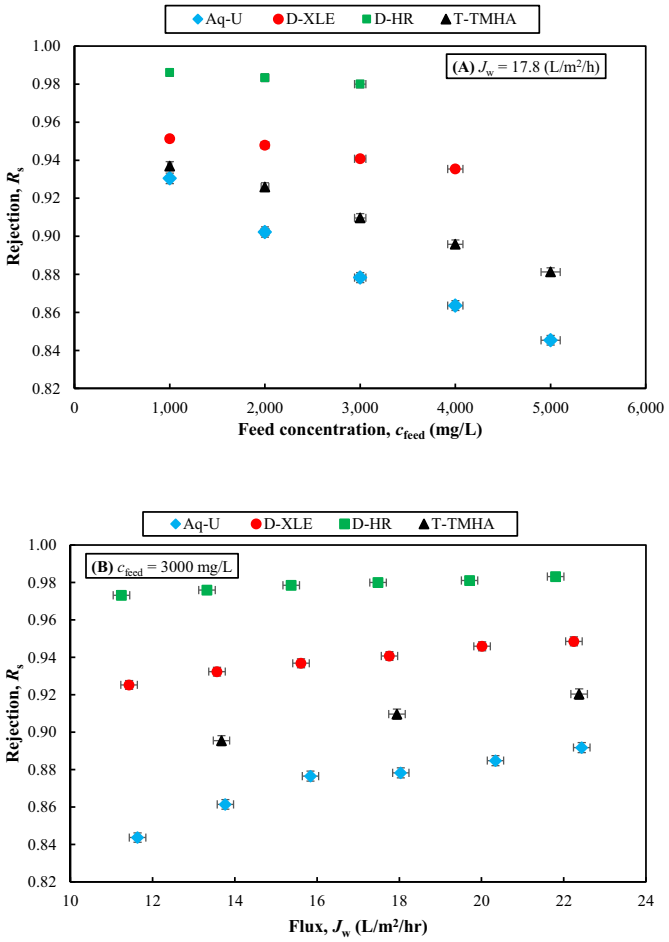

Fig. 5. Salt rejection comparison of different RO membranes, A) at J_w = 17.8 L/m^2/h and different feed concentrations, B) at c_{feed} = 3000 mg/L and different fluxes.

applications.

3.3. Salt rejection

The above permeate concentrations c_{perm} were used to calculate the salt rejection R_s of the system using the equation:

$$R_s = \frac{c_{feed} - c_{perm}}{c_{feed}} \quad (1)$$

The D-HR membrane showed the highest rejection, ranging from 97 to 99 % according to flux and feed concentration. In the case of D-XLE, rejection ranged from 91.5 to 96 %. With T-TMHA and Aq-U, the range widened considerably varying from 86 to 94.5 % and from 81.5 to 94 %

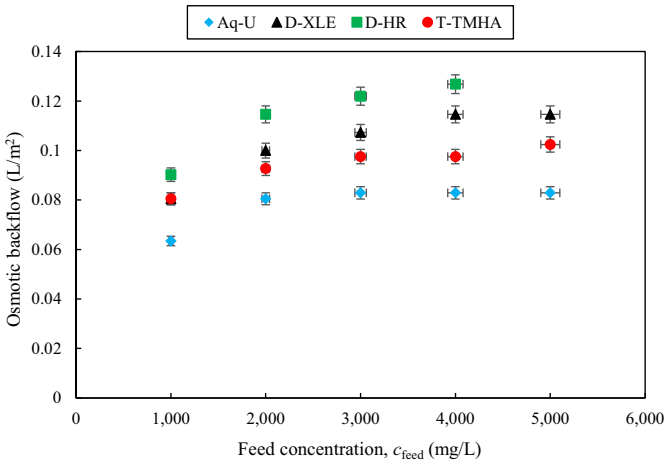

Fig. 6. Comparison of osmotic backflow per m^2 of membrane area as a function of feed concentration for different membranes at r = 0.8 and J_w = 17.8 L/m^2/h.

respectively. As an example, at c_{feed} = 2000 mg/L and J_w = 17.8 L/m^2/h, rejections were 98.3, 94.8, 92.6, and 90.2 % respectively. Figures showing the rejection for each membrane at different feed concentrations and fluxes can be found in the SI.

Rejection increased with flux but decreased with feed concentration. However, the sensitivity with the D-HR and D-XLE membranes was less than with the T-TMHA and Aq-U membranes (see Fig. 5). For instance, at J_w = 17.8 L/m^2/h, on increasing feed concentration from 1000 to 3000 mg/L, rejection of D-HR dropped by only 0.6 % while that of the Aq-U fell by 5.6 %. Additionally, at c_{feed} = 3000 mg/L, on decreasing flux from 22.2 to 11.4 L/m^2/h, rejection decreased by 1.0 and 5.4 % for D-HR and Aq-U respectively. Therefore, it may be better to operate the Aq-U and T-TMHA membranes at higher fluxes to reach higher rejection values (albeit at higher energy cost).

The rejection in the batch RO system is negatively affected by the initial peak in permeate concentration, as explained in Section 3.2 above. Moreover, comparing against the rejection values stated by the manufacturers' datasheets (Table 1) we see that, in our experiments, the flux is lower (11 to 23 L/m^2/h as opposed to 45 to 55 L/m^2/h), and the recovery is much higher (0.8 as opposed to 0.15). The feed concentration is also different. All these factors contribute to the lower rejection in the current study.

3.4. Osmotic backflow

When a batch RO system depressurizes at the beginning of the purge-and-refill phase, a small volume of permeate water fails to exit because of the osmotic backflow due to the concentration gradient [24–27]. A check valve on the permeate line helped to reduce osmotic backflow but did not eliminate it entirely.

The batch volume in this study is 69.0 L. Subtracting the batch

Table 3
Permeate and osmotic backflow volume in every batch cycle for different membranes at different feed concentrations, r = 0.8 and J_w = 17.8 L/m^2/h.

	Membrane type							
	Aq-U		D-XLE		D-HR		T-TMHA	
Feed concentration (mg/L)	Permeate volume (L)	Osmotic backflow volume (L)	Permeate volume (L)	Osmotic backflow volume (L)	Permeate volume (L)	Osmotic backflow volume (L)	Permeate volume (L)	Osmotic backflow volume (L)
1000	66.4	2.6	65.7	3.3	65.3	3.7	65.7	3.3
2000	65.7	3.3	64.9	4.1	64.3	4.7	65.2	3.8
3000	65.6	3.4	64.6	4.4	64	5	65	4
4000	65.6	3.4	64.3	4.7	63.8	5.2	65	4
5000	65.6	3.4	64.3	4.7	–	–	64.8	4.2

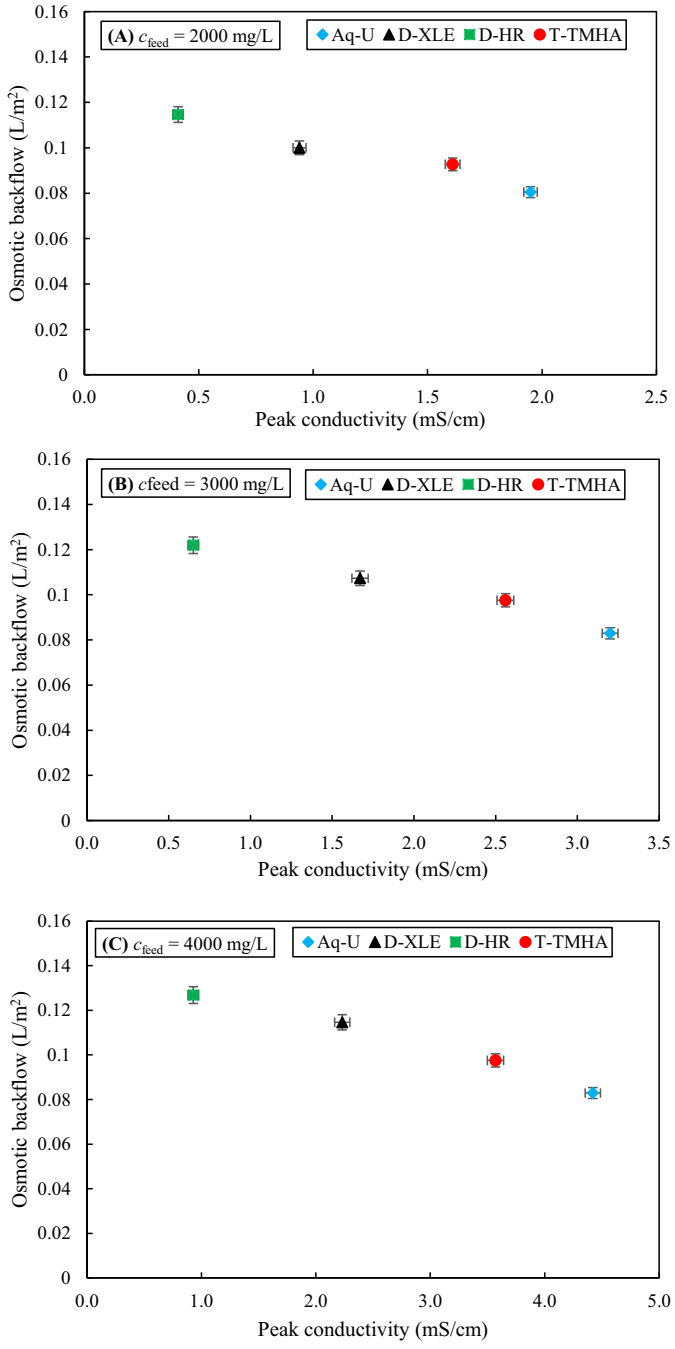

Fig. 7. Comparison of osmotic backflow per m^2 of membrane area as a function of peak conductivity for different membranes at A) c_{feed} = 2000 mg/L, B) c_{feed} = 3000 mg/L, and C) c_{feed} = 4000 mg/L, r = 0.8 and J_w = 17.8 L/m^2/h.

volume by the produced permeate volume yields the osmotic backflow, which is shown in Table 3. Osmotic backflow increased with feed concentration and varied significantly among the four membranes. The Aq-U membrane exhibited the lowest osmotic backflow volume of 2.6–3.4 L; whereas the D-HR exhibited the highest osmotic backflow volume of 3.7–5.2 L. Fig. 6 presents the results normalised to membrane area, and shows the same trend.

Comparing with the results of Section 3.3, it is interesting that membranes giving lower rejection also give lower backflow. The likely explanation is as follows. Lower rejection membranes allow more salt to pass through to the permeate. At the beginning of the purge cycle, when backflow occurs, the salt in the permeate is drawn back into the membrane support layer where it builds up as an internal concentration

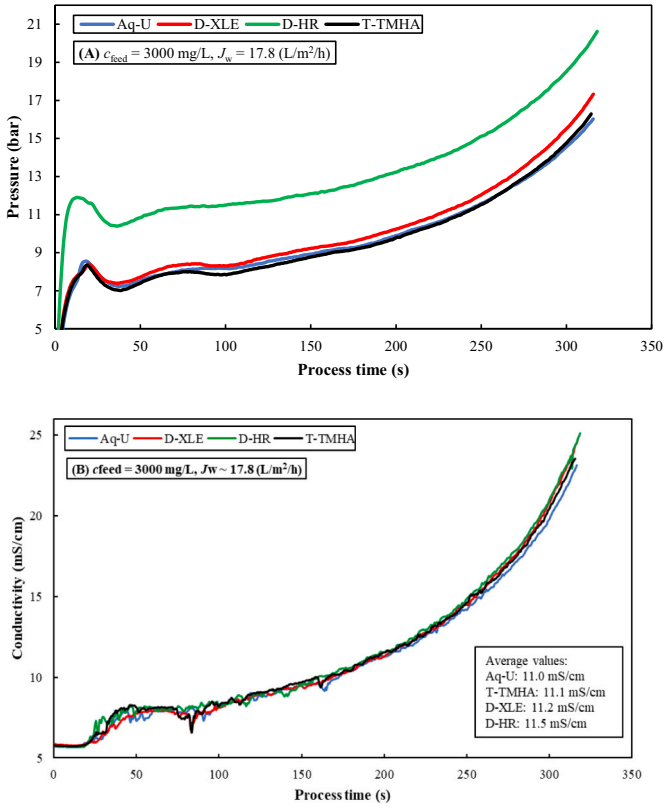

Fig. 8. Observed A) pressure, and B) inlet RO conductivity variations over a pressurization phase for different RO membranes at c_{feed} = 3000 mg/L and J_w = 17.8 L/m^2/h.

polarization (ICP) layer. Momentarily, the membrane is behaving as a forward osmosis (not reverse osmosis) membrane. It is known that the flux in forward osmosis is detrimentally affected by ICP which (unlike external concentration polarization) is not removed by convection [39]. In the case of batch RO, ICP is beneficial to reduce the backflow albeit with the penalty of lower overall salt rejection. ICP reduces the concentration gradient between the feed and permeate sides which drives osmotic backflow.

This explanation is supported by Fig. 7 which correlates the initial peak in concentration at the beginning of the permeate production against osmotic backflow. It is seen that a higher peak (associated with lower salt rejection) correlates consistently with decreased backflow. The peak reflects salt accumulation and ICP on the permeate side. The explanation is also supported by the fact that the initial peak in Fig. 3 is higher than the final peak – suggesting a multiplication of the permeate concentration by ICP during backflow prior to permeate production recommencing.

An alternative explanation could be related to the construction of the membrane element. Although the feed spacer thickness for all the membranes was the same (0.71 mm), no details were available about the permeate carrier which could hold more or less permeate according to its thickness or porosity. Nonetheless, it is unlikely that the correlation with rejection would occur just by coincidence, so the first explanation above seems much more probable.

3.5. *Pressure changes over the pressurization phase*

Fig. 8 shows how supply pump hydraulic pressure and conductivity at the RO membrane inlet vary over a batch pressurization phase at c_{feed} = 3000 mg/L and J_w = 17.8 L/m^2/h. Both variables, shown in Fig. 8(A) and (B), exhibit a similar increasing trend over the duration of the phase as the supply pump pressure increases with inlet concentration and the

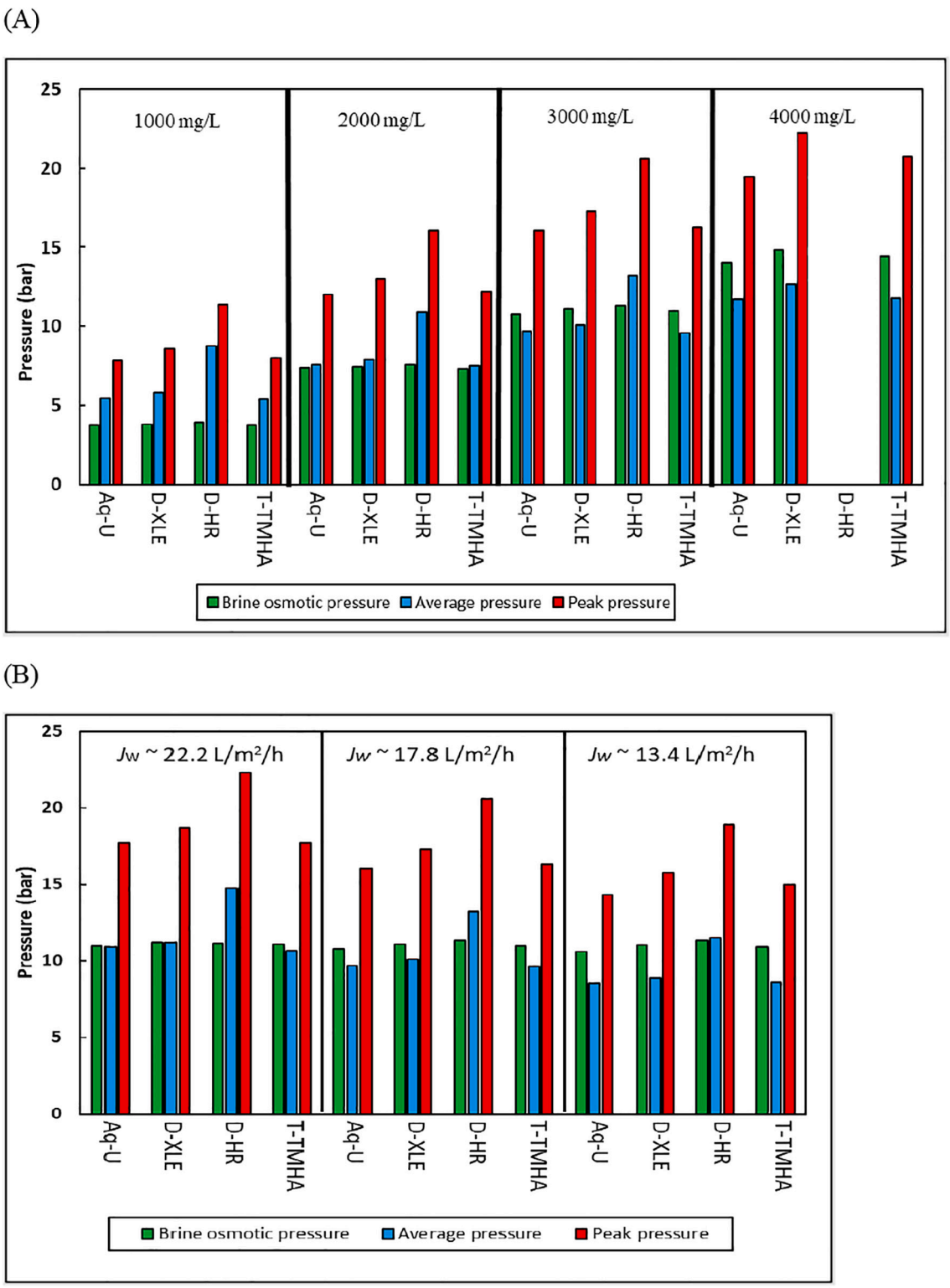

Fig. 9. Comparison of brine osmotic pressure (green), average applied pressure (blue) and peak pressure (red) of different RO membranes at A) different feed concentrations and $J_w = 17.8$ L/m^2/h, and B) different fluxes and $c_{feed} = 3000$ mg/L.

associated osmotic pressure.

The T-TMHA and Aq-U membranes demonstrated almost identical pressure trends, with average values of 9.6 and 9.7 bar, respectively. The D-XLE membrane had a slightly higher average pressure of 10.1 bar, while the high-rejection D-HR had considerably higher pressure, averaging at 13.2 bar (Fig. 8(A)). This higher pressure was caused by the lower permeability of the D-HR membrane (see Table 2).

Inlet conductivity among the four membranes was almost the same, though just slightly higher in the case of D-HR. This small difference can be explained by the higher rejection of the D-HR membrane, which resulted in more salt remaining in the recirculating loop during pressurization.

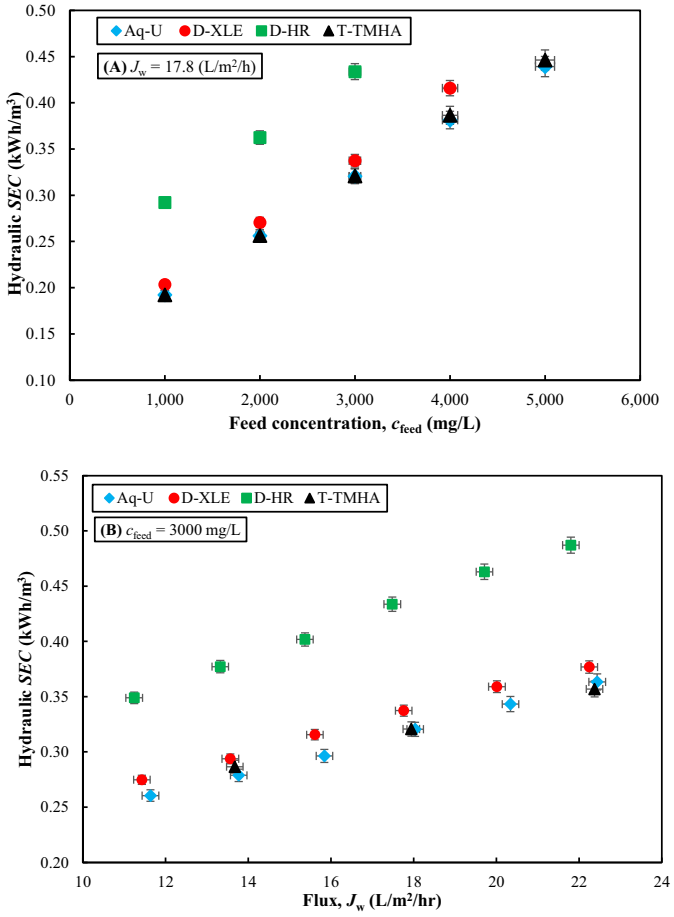

Fig. 10. Hydraulic *SEC* comparison of different RO membranes, A) at J_w = 17.8 L/m^2/h and different feed concentrations, B) at c_{feed} = 3000 mg/L and different fluxes.

3.6. Comparison of peak and average applied pressure with brine osmotic pressure

Fig. 9 compares the brine osmotic pressure, average applied pressure and peak pressure of different RO membranes at different feed concentrations and J_w = 17.8 L/m^{2}h. Brine osmotic pressure was calculated by multiplying the concentration factor (Eq. 2, derived from mass balance) by the osmotic pressure of NaCl solution calculated using the van 't Hoff expression (e.g., 0.79 bar for 1000 mg/L NaCl solution at 25 °C).

$$CF = \frac{[1 - r(1 - R_s)]}{1 - r} \quad (2)$$

Batch RO allows operation at lower average applied pressure than conventional RO. Thus, average applied pressure in batch RO can be less than the brine osmotic pressure (or exceed it by only a small margin). In contrast, in conventional RO the applied pressure must exceed the brine pressure substantially, to maintain a net driving pressure.

For the three high-permeability membranes (Aq-U, D-XLE and T-TMHA), at low feed concentration (c_{feed} < 2000 mg/L), the average applied pressure equalled or exceeded the brine osmotic pressure. This shows some deviation from the design intention – suggesting that batch RO is not so efficient in this case at recovery of 0.8. It indicates that the applied pressure requirement was dominated by membrane hydrodynamic resistance. In contrast, at feed concentration c_{feed} > 2000 mg/L, average applied pressure was lower than the brine osmotic pressure, suggesting a potential efficiency advantage over conventional RO. Nevertheless, additional factors such as osmotic backflow and recirculation pump energy usage need to be considered for a complete comparison.

For the low-permeability D-HR membrane, the average applied pressure was always higher than the brine osmotic pressure, but the gap became smaller on increasing the feed concentration. However, because of the system pressure limitation of 25 bar, we were unable to test at c_{feed} > 4000 mg/L which may have resulted in applied pressure dropping below the brine osmotic pressure.

Extending the comparison to include different fluxes (at c_{feed} = 3000 mg/L, see Fig. 9B) showed that, at decreased flux, the average applied pressure almost equalled the brine osmotic pressure with the D-HR membrane because of lower hydrodynamic resistance. All membranes showed a similar trend. Thus, on decreasing flux from 22.2 to 13.4 L/m^2/h, the difference of average applied pressure minus brine osmotic pressure decreased from −0.1, 0.0, +3.7, and − 0.5 bar, to −2.1, −2.1, +0.2, −2.3 bar for Aq-U, D-XLE, D-HR and T-TMHA membranes respectively.

Another important consideration is peak pressure. Higher pressures require more robust and expensive pressure vessels, pipework, valves, instrumentation, and other accessories. As expected, peak pressure increased with flux and feed concentration (see Fig. 9). Aq-U and T-TMHA membranes had almost similar peak pressure at various experimental conditions. The D-XLE membrane had slightly higher peak pressure, while that of D-HR membrane was much higher. For instance, at c_{feed} = 3000 mg/L and J_w = 22.2 L/m^2/h, peak pressure was about 17.7 bar when using Aq-U and T-TMHA membranes; while it increased by 5.6 % to 18.7 bar with the D-XLE membrane. The D-HR membrane gave the highest peak pressure at 21.8 bar (17 % above D-XLE and 23 % above Aq-U and T-TMHA).

3.7. Specific Energy Consumption (SEC)

Hydraulic *SEC* was measured based on the integration of differential pressure vs. discharged volume for each pump, and then totalled over the two pumps (*i.e.*, supply and recirculation pumps) and two phases of operation (*i.e.*, pressurization and purge-and-refill) as carried out previously [27]. Fig. 10 presents hydraulic *SEC* of different RO membranes at various feed concentrations and fluxes. As expected, along with the applied pressure, hydraulic *SEC* increased with flux and feed concentration. Hydraulic *SEC* was in the range 0.15–0.47 kWh/m^3 among the high-permeability membranes with only slight differences. For the high-rejection D-HR membrane, it increased to 0.21–0.48 kWh/m^3 at $c_{feed} \leq$ 4000 mg/L (and fluxes <15.5 L/m^2/h) and would likely have been higher if c_{feed} = 5000 mg/L and fluxes >15.5 L/m^2/h at c_{feed} = 4000 mg/L had been possible.

The Aq-U and T-TMHA membranes had the lowest hydraulic *SEC*, whereas that of the D-XLE membrane was slightly higher due to the lower permeability and higher rejection. The D-HR membrane had the highest hydraulic *SEC*. For example, at flux of J_w = 17.8 L/m^2/h and c_{feed} = 2000 mg/L, hydraulic *SEC* of D-HR was 0.362 kWh/m^3 while that of D-XLE was 25 % less at 0.271 kWh/m^3. That of Aq-U and T-TMHA membranes was almost the same at 0.256 kWh/m^3 (29% lower than D-HR and 6 % lower than D-XLE). On increasing the feed concentration, the gap among the membranes slightly widened, such that the hydraulic *SEC* of the T-TMHA membrane became noticeably higher than that of the Aq-U because of its greater rejection.

On almost doubling the flux, system output increased by 70 % from around 10 to 17 m^3/day. However, hydraulic *SEC* did not rise proportionately with only 35–40 % increase at c_{feed} = 3000 mg/L. Therefore, this trade-off between output and energy saving should be considered during the design and operation. Additionally, as mentioned in Section 3.2, at higher fluxes, better permeate quality is achieved.

Fig. 11 shows the electrical and hydraulic *SEC* breakdown of different RO membranes by pump and phase of operation. Most energy is used by the supply pump in the pressurization phase, providing enough pressure to overcome the osmotic pressure of feed solution and other losses in the system including major losses due to salt retention,

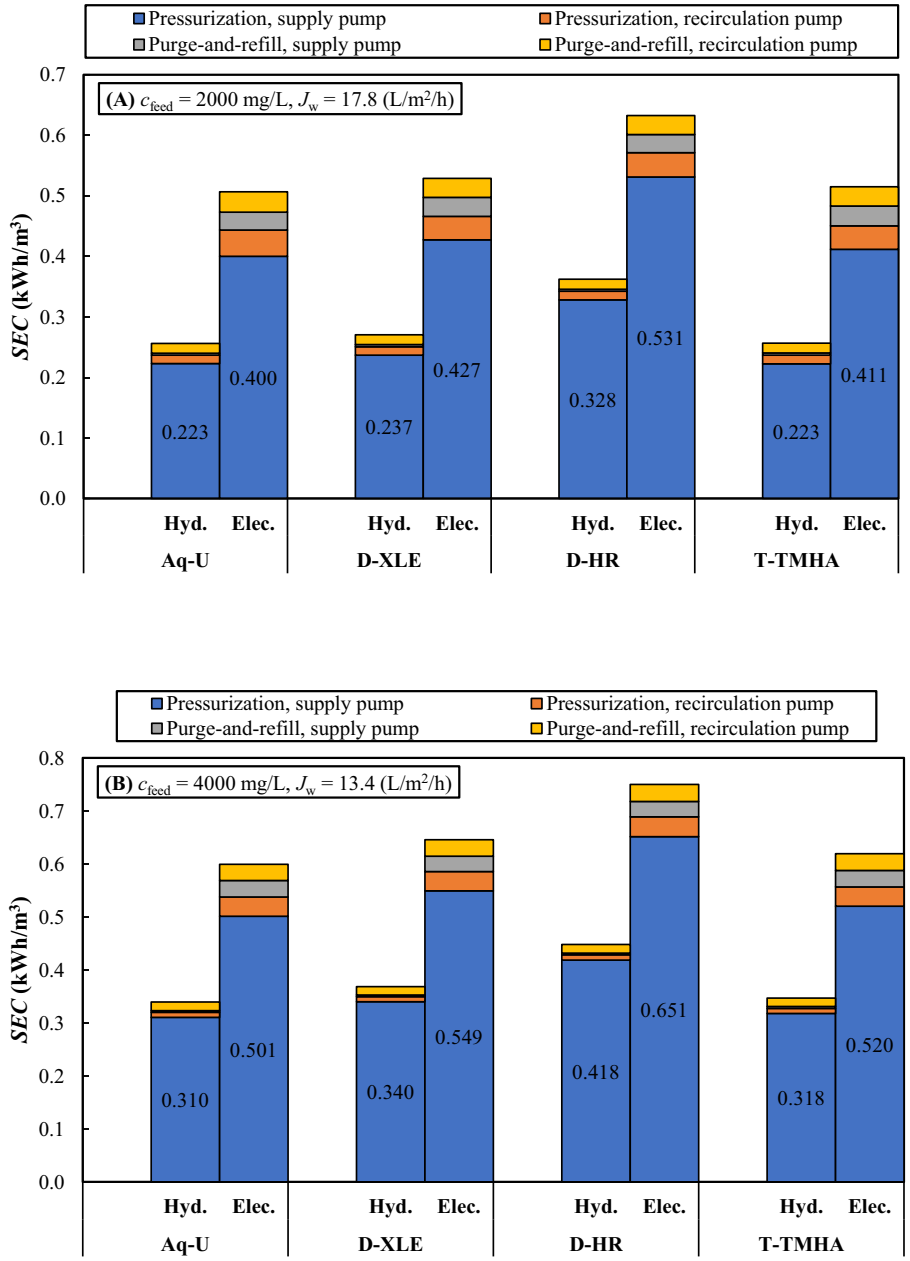

Fig. 11. Comparison of hydraulic and electrical *SEC* breakdown in batch RO system for both phases of operation and both pumps when using different RO membranes, A) at c_{feed} = 2000 mg/L, J_w = 17.8 L/m^2/h, and B) at c_{feed} = 4000 mg/L, J_w = 13.4 L/m^2/h.

concentration polarization, longitudinal concentration gradient and hydrodynamic resistance in the membrane pores.

Only 9–17 % of the total energy was consumed by the recirculation pump, with a higher percentage contribution at lower feed concentrations and fluxes when the required applied pressure is smaller. The total electrical *SEC* of the recirculation pump in all cases was around 0.06–0.065 kWh/m^3. The electrical *SEC* of the supply pump in the purge-and-refill phase was constant at around 0.03 kWh/m^3 while it varied a lot in the pressurization phase with feed concentration and flux because of variations in osmotic pressure and membrane pore resistance, respectively. As recirculation pump energy consumption is a loss in batch RO, reducing this loss is desirable for improved system performance. The loss became less significant at higher fluxes and feed concentrations.

3.8. Second law efficiency

Second law efficiency expresses the water output of a desalination system as fraction of the maximum output thermodynamically possible for a fixed energy input, while working at given operating conditions such as feed concentration, water recovery, salt rejection and temperature. As such, it enables a fair comparison among systems, regardless of the technology used and allowing for variations in operating conditions. The following equation was used to calculate second law efficiency:

$$\eta = \frac{SEC_{min}}{SEC} = \frac{\pi_{feed}\left[\frac{1}{r}ln\left(\frac{1-r[1-R_s]}{1-r}\right) - (1-R_S)ln\left(\frac{1-r[1-R_s]}{(1-r)(1-R_s)}\right)\right]}{SEC} \quad (3)$$

where electrical *SEC* is used in the denominator (*SEC* and π should be expressed in similar units [e.g. MPa] for consistency). This equation applies to a desalination system treating brackish water as used in this

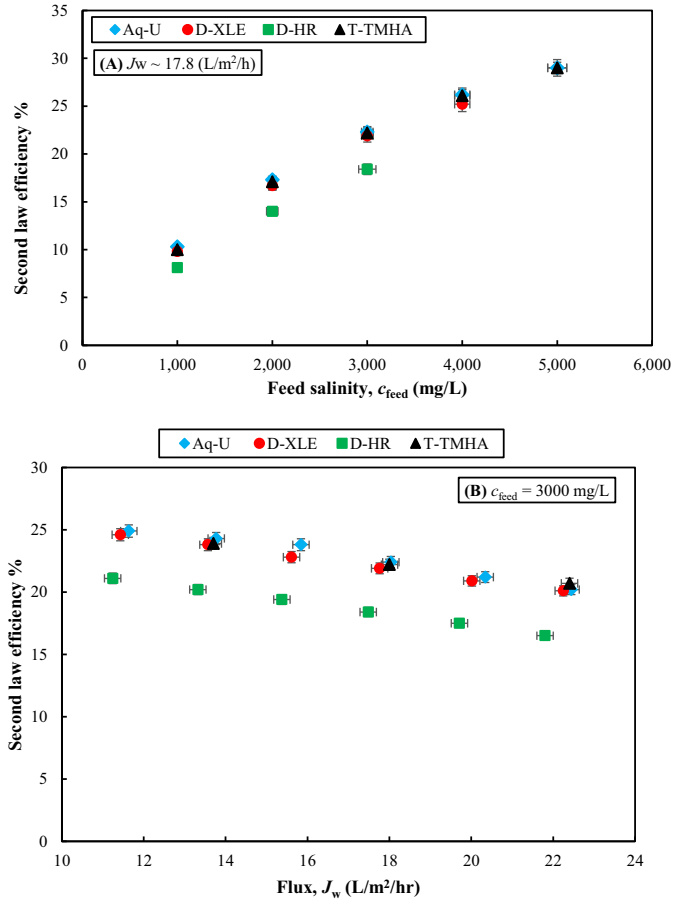

Fig. 12. Comparison of the second law efficiency of different RO membranes as a function of A) feed concentration at J_w = 17.8 L/m^2/h, and B) flux at c_{feed} = 3000 mg/L.

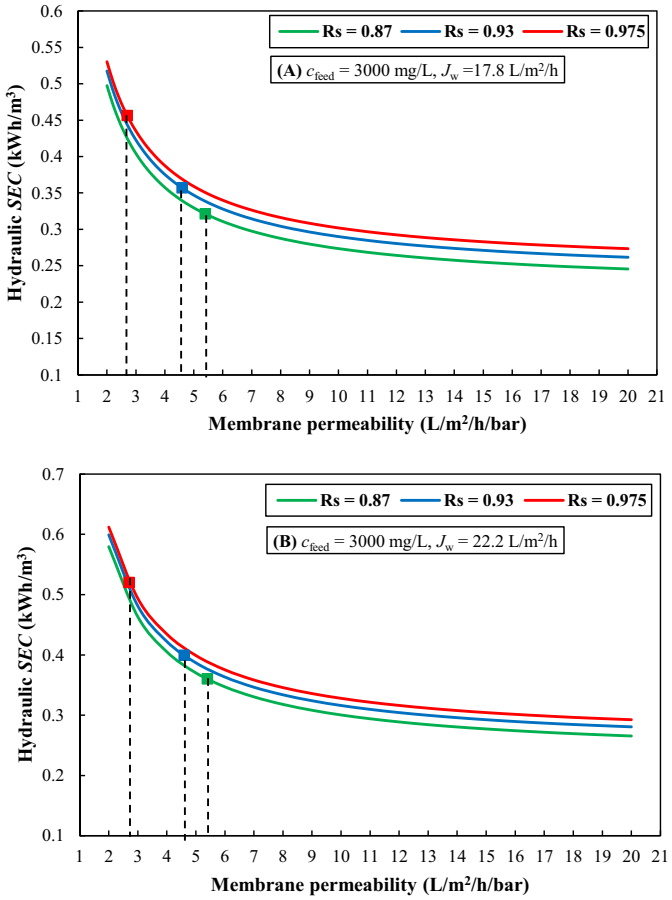

Fig. 13. Hydraulic *SEC* predictions as a function of membrane water permeability at r = 0.8, c_{feed} = 3000 mg/L and A) J_w = 17.8 L/m^2/h, and B) J_w = 22.2 L/m^2/h. The dashed lines indicate the adjusted values in model through experimental validation found in this study for D-HR, D-XLE, and Aq-U respectively from left to right.

study [40].

Fig. 12 compares second law efficiency among the different membranes as a function of flux and feed concentration. At c_{feed} = 3000 mg/L, second-law efficiencies with the Aq-U, T-TMHA and D-XLE membranes were approximately the same (21.9–22.3 %) whereas that with the D-HR membrane was slightly lower (18.4 %). Thus, the energy efficiency with the D-HR membrane lagged that of the others even with its higher rejection taken into account.

Second law efficiency increased with feed concentration and decreased with flux. Over the whole range of concentrations and fluxes used in this study, the lowest second law efficiency of 7 % occurred with D-HR at the lowest feed concentration and highest flux (c_{feed} = 1000 mg/L and J_w = 22.2 L/m^2/h); the highest was about 31 % at the highest feed concentration and lowest flux (c_{feed} = 5000 mg/L and J_w = 11.4 L/m^2/h) for the high permeability membranes.

As reported in [26], second law efficiency of some of the existing brackish RO plants [41–44] are in the range of 1.5 to 4.5 % when they supplied with feed concentrations of 900–2500 mg/L and operate at high recoveries (ranging from 0.6 to 0.8). Compared to these plants, under nearly similar conditions, batch RO showed higher second law efficiency, ranging between 8 and 22 % with high-permeability membranes and 7–19 % with the low-permeability membrane.

4. Reduction in *SEC* through future membrane improvements

RO membranes have undergone a steady enhancement in permeability over the past few decades while maintaining their selectivity [4,45]. This trend is anticipated to continue with further advances in membrane materials and manufacturing techniques. In this section, a verified model [25,27] is used to project reductions in *SEC* that would result from future ultra-high permeability membranes. Details of the modelling assumptions and verification can be found in the SI and the model spreadsheet is provided as a supplementary file.

Projections are made of *SEC* with increasing permeability for different cases of rejection and osmotic backflow. Recovery is kept at 0.8, with feed concentrations of 3000 and 5000 mg/L and fluxes of 17.8 and 22.2 L/m^2/h. For a high-rejection membrane with R_s = 0.975 and osmotic backflow of 5.0 L (i.e., similar to the D-HR membrane) predictions at J_w = 17.8 L/m^2/h show that increasing permeability from 2.7 to 10 and 20 L/m^2/h/bar would reduce *SEC* by 34 % and 40 % respectively, giving *SEC*s of 0.302 and 0.273 kWh/m^3 compared to 0.456 kWh/m^3 at 2.7 L/m^2/h/bar. This *SEC* reduction will be even greater at higher fluxes. For instance, at slightly higher flux (J_w = 22.2 L/m^2/h), *SEC* would be 37 % and 44 % less at 10 and 20 L/m^2/h/bar respectively, compared to that at permeability of 2.7 L/m^2/h/bar (see Fig. 13). This improvement corresponds to an increase in the second law efficiency from 22.3 % to 35.1 % and 38.7 % respectively (assuming 80 % efficiency for both pumps).

For a high-permeability low-rejection membrane with R_s = 0.87 and osmotic backflow of 3.4 L (i.e., similar to the Aq-U membrane) predictions at J_w = 17.8 L/m^2/h indicate that doubling the water permeability from 5 to 10 L/m^2/h/bar, results in approximately 17 % *SEC* reduction. At 20 L/m^2/h/bar, *SEC* is predicted to drop further by 25 %. At higher flux (J_w = 22.2 L/m^2/h) these reductions further improve to 19 % and 28 % respectively (see Fig. 13), corresponding to second law

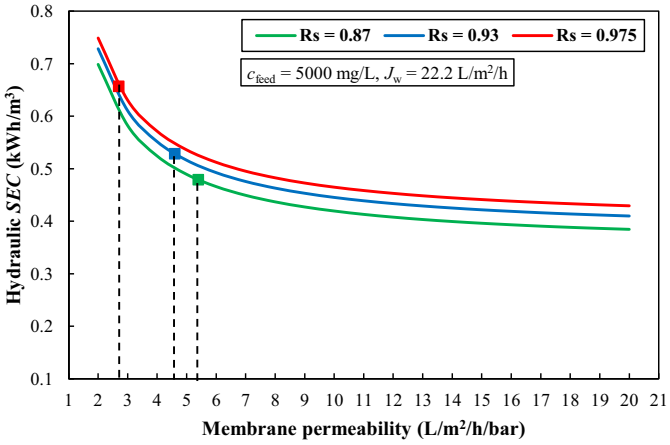

Fig. 14. Hydraulic *SEC* predictions as a function of membrane water permeability at $r = 0.8$, $c_{feed} = 5000$ mg/L and $J_w = 22.2$ L/m^2/h. The dashed lines indicate the adjusted values in model through experimental validation found in this study for D-HR, D-XLE, and Aq-U respectively from left to right.

efficiencies of 37.7 and 42 %.

Predictions also show that energy savings resulting from enhanced membrane water permeability decrease as the feed concentration increases. For instance, on permeability increase from 2.7 to 10 L/m^2/h/bar in the case of the low-permeability high-rejection membrane ($R_s = 0.975$), *SEC* falls by 29 % at $c_{feed} = 5000$ mg/L (see Fig. 14), compared to 37 % at 3000 mg/L. In the case of the high-permeability low-rejection membrane ($R_s = 0.87$), increasing permeability from 5 to 10 L/m^2/h/bar results in 14 % *SEC* reduction at $c_{feed} = 5000$ and 19 % reduction at $c_{feed} = 3000$ mg/L.

Predictions in this study show that, in contrast to previous studies regarding continuous RO, increasing permeability still has an important role in *SEC* reduction in batch RO. When using single-stage ROs, 5 and 8 L/m^2/h/bar was predicted as the upper limit of useful permeability for the *SEC* reduction in BWRO by Cohen-Tanugi et al. [16] and Okamoto and Lienhard [3] respectively. However, we predict about 16 % *SEC* reduction at 20 L/m^2/h/bar compared to 8 L/m^2/h/bar.

Moreover, Werber et al. [17] reported only a 2.2 % energy saving on increasing permeability from 4 to 10 L/m^2/h/bar in single-stage BWRO while the energy saving was about 12 % (0.05 kWh/m^3) in a two-stage RO system. In contrast, our predictions suggest a more substantial reduction in *SEC* (up to 20 %, equivalent to 0.11 kWh/m^3) in the batch RO system under almost similar conditions.

Comparing to previous studies of batch RO, Warsinger et al. [34] reported a 40 % reduction in energy consumption when increasing membrane permeability from 1 to 10 L/m^2/h/bar, with a 37 % saving observed before reaching 7 L/m^2/h/bar. Our predictions indicate a slightly higher 59 % reduction in *SEC* on going from 1 to 10 L/m^2/h/bar. Both studies agree, however, that the *SEC* reduction in the permeability range of 7 to 10 L/m^2/h/bar is <10 %.

Table 4 summarises and compares the most relevant studies on *SEC* reduction resulting from use of higher permeability membranes. We note that caution is needed in comparing the studies because of the variations in operating conditions and assumptions used among the studies.

5. Conclusion

We experimentally investigated the performance of a free-piston batch RO system using four different 8-in. RO membranes of differing water permeability, thus evaluating the effect of permeability on salt rejection, permeate quality, *SEC,* and efficiency. Permeability of the membranes was measured and found to be in the range of 2.7–5.7 L/m^2/h/bar.

The system was tested at recovery of 0.8 with brackish water feed

Table 4
Simulation conditions from various references assessing the relationship between membrane permeability and SEC in brackish water RO desalination.

Author	Configuration	Feed concentration (mg/L)	Recovery	Flux (L/m^2/h)	Rejection (%)	Pump efficiency (%)	ERD efficiency (%)	Key findings	Reference
Cohen-Tanugi et al.	Continuous RO	2000	0.65	13.2	99.8	75	97	47 % decrease in feed pump pressure when permeability increases from 1.5 to 4.5 L/m^2/h/bar. 5 L/m^2/h/bar was considered as a meaningful limit for SEC reduction.	[16]
Shrivastava et al.	Continuous RO	804	0.85	N.D.	N.D.	85	95	30 % decrease in SEC when permeability increases from 2.5 to 5 L/m^2/h/bar.	[46]
Werber et al.	Continuous RO	5844	0.75	15	N.D.*	100	100	2.2 % SEC reduction in single-stage while 12 % SEC reduction in two-stage when permeability increases from 4 to 10 L/m^2/h/bar. They stated that the reason for minor SEC reduction is that the hydraulic overpressure is small.	[17]
Wei et al.	Continuous RO	3000	0.6–0.98	15	100	100	100	SEC saving of 0.02 kWh/m^3 at low recovery of 0.6 when permeability increases from 1 to 10 L/m^2/h/bar. At very high recoveries of 0.98, SEC became almost insensitive to permeability.	[19]
Karabelas et al.	Continuous RO	2000	0.7	N.D.	N.D.	85	95	51.2 % of SEC is related to membrane filtration resistance and can be reduced by improved membrane permeability.	[47]
Warsinger et al.	Batch RO	5000	0.66	14.5	N.D.**	80	N.D.	About 40 % SEC reduction when increasing permeability from 1 to 10 L/m^2/h/bar.	[34]
Current study	Batch RO	3000 & 5000	0.8	17.8 & 22.2	0.87 and 0.93 and 0.975	100	N.A.	59–67 % SEC reduction when increasing permeability from 1 to 10 L/m^2/h/bar.	–

* B-value was used.
** All scenarios were assumed to have the same permeate quality.

containing 1000–5000 mg/L of NaCl, at fluxes of about 11–23 L/m^2/h. Whereas salt rejection with the low-permeability membrane varied little from 97 to 99 %, that with the three high-permeability membranes varied more widely from 82 to 96 %, with the lowest rejections seen at lowest fluxes and greatest feed concentrations. All membranes achieved an acceptable permeate quality for drinking and irrigation applications. However, for high-permeability membranes, operation at higher fluxes (> 14 L/m^2/h) is necessary at high feed concentrations (> 5000 mg/L) to ensure water quality standards are met - albeit at the expense of slightly higher energy consumption.

We observed significant variations in osmotic backflow volume among the membranes and according to the feed salinity. The lower backflow (of 2.6 L) occurred with the lowest rejection membrane at low feed salinity of 1000 mg/L, whereas the highest (of 5.2 L) occurred with the highest rejection membrane at feed salinity of 4000 mg/L.

When comparing the hydraulic *SEC* among the four membranes, that obtained using the high-permeability membranes was considerably lower than with the low-permeability membrane (D-HR). For example, at feed concentration of 2000 mg/L and flux of 17.8 L/m^2/h, hydraulic *SEC* using the high-permeability membranes was 25–29 % lower than obtained using the D-HR membrane.

Second law efficiency of up to 31 % was achieved, comparing favourably to existing brackish water RO plants. This could increase to 42 % with improvements in membrane permeability. At higher feed concentrations, the average applied pressure was lower than the brine osmotic pressure exiting the system - thus indicating improved energy performance against single-stage continuous RO.

Unlike several earlier studies of continuous RO [3,16,17,19], this study predicts that increasing permeability to values of 10 or 20 L/m^2/h/bar will continue to have benefits in reducing *SEC* in batch RO. On increasing permeability from the baseline value of 2.7 L/m^2/h/bar to 10 and 20 L/m^2/h/bar, we predict *SEC* reductions of 37 and 44 % respectively for a high-rejection membrane (R_s = 0.975). For a low-rejection membrane (R_s = 0.87), with baseline permeability of 5.4 L/m^2/h/bar, we predict corresponding reductions of 17 and 28 % (at 10 and 20 L/m^2/h/bar respectively) at feed concentration of 3000 mg/L and flux of 22.2 L/m^2/h. The energy savings would be even greater at higher fluxes and lower feed concentrations. This highlights the on-going importance of research into new materials and techniques of membrane fabrication to increase water permeability. There is also a need for economic studies to assess the costs and benefits of developing and implementing future high-permeability membranes in batch RO.

CRediT authorship contribution statement

E. Hosseinipour: Writing – original draft, Investigation, Formal analysis, Methodology. **P.A. Davies:** Writing – review & editing, Supervision, Resources, Methodology, Conceptualization.

Declaration of competing interest

The authors would like to declare that a spinout company has been formed to exploit the batch RO technology described in this article, and that one of the authors (PAD) has an equity stake in the spinout company.

Data availability

Data will be made available on request.

Acknowledgements

This project has received funding from the European Union's Horizon 2020 research and innovation programme under grant agreement No 820906. We would also like to acknowledge valuable contributions by Dr. Jörg Vogel of Aquaporin A/S (Denmark) in advising about and supplying membranes. The authors would also like to thank Rubén Rodríguez Alegre for his comments and corrections on the manuscript.

Appendix A. Supplementary data

Supplementary data to this article can be found online at https://doi.org/10.1016/j.desal.2024.117378.

References

[1] A. Yusuf, A. Sodiq, A. Giwa, J. Eke, O. Pikuda, G. De Luca, J.L. Di Salvo, S. Chakraborty, A review of emerging trends in membrane science and technology for sustainable water treatment, J. Clean. Prod. 266 (2020) 121867.
[2] S.S. Shenvi, A.M. Isloor, A. Ismail, A review on RO membrane technology: developments and challenges, Desalination 368 (2015) 10–26.
[3] Y. Okamoto, J.H. Lienhard, How RO membrane permeability and other performance factors affect process cost and energy use: a review, Desalination 470 (2019) 114064.
[4] R.H. Hailemariam, Y.C. Woo, M.M. Damtie, B.C. Kim, K.-D. Park, J.-S. Choi, Reverse osmosis membrane fabrication and modification technologies and future trends: a review, Adv. Colloid Interf. Sci. 276 (2020) 102100.
[5] Z. Yang, X.-H. Ma, C.Y. Tang, Recent development of novel membranes for desalination, Desalination 434 (2018) 37–59.
[6] D. Li, Y. Yan, H. Wang, Recent advances in polymer and polymer composite membranes for reverse and forward osmosis processes, Prog. Polym. Sci. 61 (2016) 104–155.
[7] L.F. Greenlee, D.F. Lawler, B.D. Freeman, B. Marrot, P. Moulin, Reverse osmosis desalination: water sources, technology, and today's challenges, Water Res. 43 (2009) 2317–2348.
[8] H.B. Park, C.H. Jung, Y.M. Lee, A.J. Hill, S.J. Pas, S.T. Mudie, E. Van Wagner, B. D. Freeman, D.J. Cookson, Polymers with cavities tuned for fast selective transport of small molecules and ions, Science 318 (2007) 254–258.
[9] M. Bekbolet, C. Uyguner, H. Selcuk, L. Rizzo, A. Nikolaou, S. Meric, V. Belgiorno, Application of oxidative removal of NOM to drinking water and formation of disinfection by-products, Desalination 176 (2005) 155–166.
[10] D. Qadir, H. Mukhtar, L.K. Keong, Mixed matrix membranes for water purification applications, Sep. Purif. Rev. 46 (2017) 62–80.
[11] M. Aroon, A. Ismail, T. Matsuura, M. Montazer-Rahmati, Performance studies of mixed matrix membranes for gas separation: a review, Sep. Purif. Technol. 75 (2010) 229–242.
[12] M. Wang, Z. Wang, X. Wang, S. Wang, W. Ding, C. Gao, Layer-by-layer assembly of aquaporin Z-incorporated biomimetic membranes for water purification, Environ. Sci. Technol. 49 (2015) 3761–3768.
[13] M. Grzelakowski, M.F. Cherenet, Y.-X. Shen, M. Kumar, A framework for accurate evaluation of the promise of aquaporin based biomimetic membranes, J. Membr. Sci. 479 (2015) 223–231.
[14] L. Sharma, L. Ye, C. Yong, R. Seetharaman, K. Kho, W. Surya, R. Wang, J. Torres, Aquaporin-based membranes made by interfacial polymerization in hollow fibers: visualization and role of aquaporin in water permeability, J. Membr. Sci. 654 (2022) 120551.
[15] J.R. Werber, C.O. Osuji, M. Elimelech, Materials for next-generation desalination and water purification membranes, Nat. Rev. Mater. 1 (2016) 1–15.
[16] D. Cohen-Tanugi, R.K. McGovern, S.H. Dave, J.H. Lienhard, J.C. Grossman, Quantifying the potential of ultra-permeable membranes for water desalination, Energy Environ. Sci. 7 (2014) 1134–1141.
[17] J.R. Werber, A. Deshmukh, M. Elimelech, The critical need for increased selectivity, not increased water permeability, for desalination membranes, Environ. Sci. Technol. Lett. 3 (2016) 112–120.
[18] A. Zhu, P.D. Christofides, Y. Cohen, Energy consumption optimization of reverse osmosis membrane water desalination subject to feed salinity fluctuation, Ind. Eng. Chem. Res. 48 (2009) 9581–9589.
[19] Q.J. Wei, R.K. McGovern, J.H. Lienhard, Saving energy with an optimized two-stage reverse osmosis system, Environ. Sci.: Water Res. Technol. 3 (2017) 659–670.
[20] P.A. Davies, J. Wayman, C. Alatta, K. Nguyen, J. Orfi, A desalination system with efficiency approaching the theoretical limits, Desalin. Water Treat. 57 (2016) 23206–23216.
[21] K. Park, L. Burlace, N. Dhakal, A. Mudgal, N.A. Stewart, P.A. Davies, Design, modelling and optimisation of a batch reverse osmosis (RO) desalination system using a free piston for brackish water treatment, Desalination 494 (2020) 114625.
[22] D.M. Warsinger, E.W. Tow, K.G. Nayar, L.A. Maswadeh, J.H. Lienhard, Energy efficiency of batch and semi-batch (CCRO) reverse osmosis desalination, Water Res. 106 (2016) 272–282.
[23] J.R. Werber, A. Deshmukh, M. Elimelech, Can batch or semi-batch processes save energy in reverse-osmosis desalination? Desalination 402 (2017) 109–122.
[24] Q.J. Wei, C.I. Tucker, P.J. Wu, A.M. Trueworthy, E.W. Tow, J.H. Lienhard, Impact of salt retention on true batch reverse osmosis energy consumption: experiments and model validation, Desalination 479 (2020) 114177.
[25] E. Hosseinipour, E. Harris, H.A. El Nazer, Y.M. Mohamed, P.A. Davies, Desalination by batch reverse osmosis (RO) of brackish groundwater containing sparingly soluble salts, Desalination 566 (2023) 116875.
[26] E. Hosseinipour, S. Karimi, S. Barbe, K. Park, P.A. Davies, Hybrid semi-batch/batch reverse osmosis (HSBRO) for use in zero liquid discharge (ZLD) applications, Desalination 544 (2022) 116126.

[27] E. Hosseinipour, K. Park, L. Burlace, T. Naughton, P.A. Davies, A free-piston batch reverse osmosis (RO) system for brackish water desalination: experimental study and model validation, Desalination 527 (2022) 115524.
[28] M. Elimelech, W.A. Phillip, The future of seawater desalination: energy, technology, and the environment, Science 333 (2011) 712–717.
[29] D.M. Davenport, C.L. Ritt, R. Verbeke, M. Dickmann, W. Egger, I.F. Vankelecom, M. Elimelech, Thin film composite membrane compaction in high-pressure reverse osmosis, J. Membr. Sci. 610 (2020) 118268.
[30] M. Aghajani, M. Wang, L.M. Cox, J.P. Killgore, A.R. Greenberg, Y. Ding, Influence of support-layer deformation on the intrinsic resistance of thin film composite membranes, J. Membr. Sci. 567 (2018) 49–57.
[31] J.A. Idarraga-Mora, A.D. O'Neal, M.E. Pfeiler, D.A. Ladner, S.M. Husson, Effect of mechanical strain on the transport properties of thin-film composite membranes used in osmotic processes, J. Membr. Sci. 615 (2020) 118488.
[32] M. Askari, C.Z. Liang, L.T.S. Choong, T.-S. Chung, Optimization of TFC-PES hollow fiber membranes for reverse osmosis (RO) and osmotically assisted reverse osmosis (OARO) applications, J. Membr. Sci. 625 (2021) 119156.
[33] S. Cordoba, A. Das, J. Leon, J.M. Garcia, D.M. Warsinger, Double-acting batch reverse osmosis configuration for best-in-class efficiency and low downtime, Desalination 506 (2021) 114959.
[34] D.M. Warsinger, J. Swaminathan, J.H. Lienhard, Ultrapermeable Membranes for Batch Desalination: Maximum Desalination Energy Efficiency, and Cost Analysis, 2017.
[35] J. Swaminathan, R. Stover, E.W. Tow, D.M. Warsinger, J.H. Lienhard, Effect of practical losses on optimal design of batch RO systems, 2017.
[36] P. Khunnonkwao, K. Jantama, S. Kanchanatawee, S. Galier, H. Roux-de Balmann, A two steps membrane process for the recovery of succinic acid from fermentation broth, Sep. Purif. Technol. 207 (2018) 451–460.
[37] P.A. Davies, A.K. Hossain, Development of an integrated reverse osmosis-greenhouse system driven by solar photovoltaic generators, Desalin. Water Treat. 22 (2010) 161–173.
[38] W.H. Organization, Guidelines for Drinking-Water Quality: Incorporating the First and Second Addenda, World Health Organization, 2022.
[39] M. Mohammadifakhr, J. de Grooth, H.D. Roesink, A.J. Kemperman, Forward osmosis: a critical review, Processes 8 (2020) 404.
[40] L. Wang, C. Violet, R.M. DuChanois, M. Elimelech, Derivation of the theoretical minimum energy of separation of desalination processes, J. Chem. Educ. 97 (2020) 4361–4369.
[41] N. Kahraman, Y.A. Cengel, B. Wood, Y. Cerci, Exergy analysis of a combined RO, NF, andEDR desalination plant, Desalination 171 (2005) 217–232.
[42] I.H. Aljundi, Second-law analysis of a reverse osmosis plant in Jordan, Desalination 239 (2009) 207–215.
[43] M.H. Sharqawy, S.M. Zubair, Second law analysis of reverse osmosis desalination plants: an alternative design using pressure retarded osmosis, Energy 36 (2011) 6617–6626.
[44] A.A. Alsarayreh, M.A. Al-Obaidi, A. Ruiz-García, R. Patel, I.M. Mujtaba, Thermodynamic limitations and exergy analysis of brackish water reverse osmosis desalination process, Membranes 12 (2021) 11.
[45] Y.J. Lim, K. Goh, M. Kurihara, R. Wang, Seawater desalination by reverse osmosis: current development and future challenges in membrane fabrication–a review, J. Membr. Sci. 629 (2021) 119292.
[46] A. Shrivastava, S. Rosenberg, M. Peery, Energy efficiency breakdown of reverse osmosis and its implications on future innovation roadmap for desalination, Desalination 368 (2015) 181–192.
[47] A. Karabelas, C. Koutsou, M. Kostoglou, D. Sioutopoulos, Analysis of specific energy consumption in reverse osmosis desalination processes, Desalination 431 (2018) 15–21.